Inert Gas Test of Two 12-cm Magnetostatic Thrusters

William D. Ramsey*
Loral Electro-Optical Systems,† Pasadena, California

Comparative performance tests were conducted with 12-cm-diam line and ring magnetic cusp thrusters. Shell anode and magnetoelectrostatic containment boundary anode configurations were evaluated with each magnet array. The best performance was achieved with the ring cusp-shell anode configuration. Argon operation of this configuration produced 65-81% mass utilization efficiency at 170-208 W/single-charge-equivalent (SCE) ampere beam. Xenon test results showed 75-95% utilization at 162-188 W/SCE ampere beam.

Introduction

THIS paper describes the continuing development of midsize, 12-cm-diam, inert gas ion thrusters.[1,2] The development emphasized improvements in discharge chamber performance or reduction in the discharge power needed to ionize the majority of the propellant flow. Performance tests were conducted with two types of discharge chambers using two anode configurations.

The magnetoelectrostatic containment (MESC) anode configuration was first described and tested by Moore.[3] His test results showed the MESC configuration had excellent cesium performance. These results were later used in the design of a thruster system experiment tested at geosynchronous orbit aboard Application Technology Satellite 6.[4] Moore's original 12-cm discharge chamber was later modified for mercury operation and produced excellent performance.[5] The first MESC inert gas development program further modified the original thruster.[1]

Briefly stated, Moore's MESC design consisted of magnets and anode rings. The magnets were arranged in rings inside an iron discharge chamber with the plane of each ring cusp orthogonal to the chamber centerline. The rings were magnetized normal to the chamber wall. Adjacent rings alternated in polarity to create a field over the anodes between the magnets. The shell assembly operated at cathode potential.

The shell anode, or second anode configuration, was first reported by Sovey.[6] The shell anode chamber consisted of the MESC magnet pattern without anode rings. The entire chamber or shell functioned as the anode and was electrically isolated from the screen grid and cathode hardware. Sovey reported good inert gas performance was obtained with the magnet pattern arranged in rows parallel to the chamber centerline or in a line cusp. He has since tested a ring cusp-shell anode thruster.[7]

Apparatus

Thruster Components

Two 12-cm thruster types and two anode configurations were tested in this effort. The line cusp and ring cusp thruster each were tested in MESC boundary anode and shell anode configurations. Although each thruster type was a different discharge chamber assembly, they were tested with the same hollow cathode and ion optic subassemblies. The commonality minimized the possibility of introducing errors in the performance comparison and expedited test turnaround.

The 6.4-mm hollow cathode subassembly consisted of a cathode with a 0.5-mm-diam countersunk orifice, a keeper, and a baffle. The baffle was a 1.3×0.47 cm i.d. tantalum washer as opposed to the solid disk used in previously reported tests.[2] The washer was located 1.1 cm downstream of the cathode as shown in Fig. 1. The washer baffle operated at keeper potential.

Line Cusp Thruster

The line cusp discharge chamber was divided into two sections for easy fabrication, as shown in Fig. 2. A 2.3-cm-long conical section adapted the main portion of the discharge chamber to the cathode magnet diameter. The 24 magnet rows in the cone were parallel to the chamber centerline and varied in length. The longer rows had the same polarity as the cathode magnet. The cathode-baffle subassembly could be electrically isolated from the discharge chamber assembly.

The cylindrical main discharge section contained a matching 24 rows of alternating polarity magnets. Aluminum-nickel-cobalt (alnico) magnets with 0.17 T residual fields were used throughout.

In the MESC configuration a two-piece anode row was located between each pair of magnets. In the shell anode configuration tests, the anodes were removed and the discharge chamber assembly was isolated from the screen grid. During shell anode operation, the screen grid and cathode were tied together electrically while the magnet-chamber assembly operated at anode potential.

Ring Cusp Thruster

The ring cusp discharge chamber is described in Ref. 2. MESC configuration tests were conducted with six cusps of alnico magnets evenly spaced along the chamber walls.

Different magnet materials distinguished two series of ring cusp shell anode tests. The first series was conducted with 6, 4, and 2 cusp configurations of the alnico magnets. The second series of shell anode tests was conducted with 4 and 2 cusps of samarium-cobalt magnets. These magnets had the same physical dimensions as the alnico but greater, 0.27 T, residual fields.

Discharge Probes

Ion current distribution to the magnets and walls of the ring cusp shell anode configuration was measured with 0.64 cm^2 pieces of tantalum foil. The foil pieces were mounted on insulators and located 2.0 mm radially from the magnets and walls.

E × B Probe

The majority of the double-charged ion beam data were collected with an E × B probe located ~15 cm from the decel grid. The probe and its operation are described in a previous paper by Vahrenkamp.[8] Only centerline data were collected to expedite testing and give a "worst-case" approximation to the

Presented as Paper 82-1925 at the AIAA/JSASS/DGLR 16th International Electric Propulsion Conference, New Orleans, La., Nov. 17-19, 1982; received Dec. 13, 1982; revision received Feb. 26, 1984.

*Physicist. Member AIAA.
†Formerly Xerox Electro-Optical Systems.

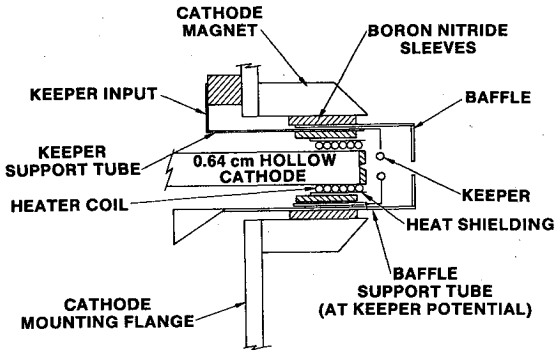

Fig. 1 Cathode subassembly.

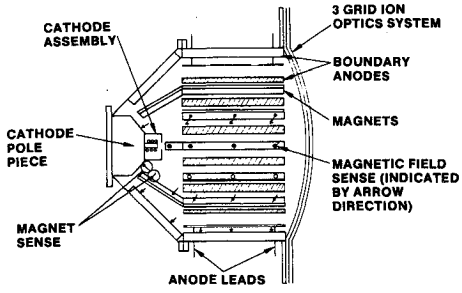

Fig. 2 12-cm line cusp MESC configuration.

percentage of double-charged beam ions. The centerline probe data were found to agree with time-of-flight collector results. The time-of-flight collector is described in Ref. 1. The double-charged ion data were used to correct the ion beam to single-charged equivalent (SCE) for mass efficiency and discharge power calculations.

Test Results

Discharge Chamber Optimization

The underlying principle of performance optimization was the same for the MESC and shell anode configurations. Optimization consisted of reducing the anode area until futher reduction made the discharge difficult to start and/or caused discharge oscillation at nominal operational parameters or reduced performance.

MESC anode area was controlled by varying the anode magnetic field[9] or the number of anodes in the discharge chamber. Increases in anode magnetic field reduced the area by reducing the Larmor radius of the electrons reaching the anodes.[10]

Shell anode discharge optimization followed the same logic. Since the magnet faces served as anodes in this configuration,[10] area reduction meant removing magnet rows or substituting stronger magnets in place of the existing ones.

Line Cusp Thruster Performance

The best performance achieved in the line cusp thruster tests with MESC or shell anode configurations are shown in Figs. 3 and 4. The shell anode configuration had better argon performance achieving 50-74% mass utilization efficiency at 300-340 W/SCE ampere beam. This is 50 W/SCE ampere beam better argon performance than the line cusp MESC configuration. MESC xenon performance achieved 50-87% utilization at ~300 W/SCE ampere beam. No complete set of shell anode xenon performance data was collected.

Five different anode magnetic fields were performance mapped in the line cusp MESC configuration tests. The best performance was produced by locating adjacent anodes in alternating high and low boundary magnetic fields. One set of 12 anode rows (set 1) was located in an 18.0 mT field interspersed with 12 rows (set 2) in a 12.0 mT field. An examination of the electron distribution seen in the different

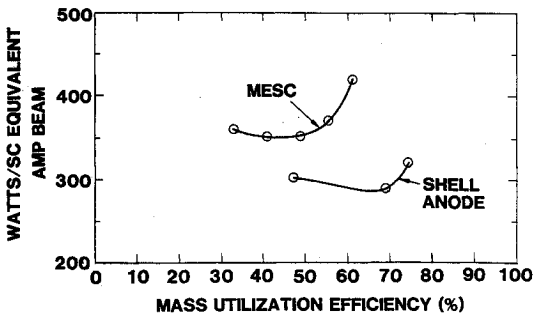

Fig. 3 Line cusp thruster argon performance.

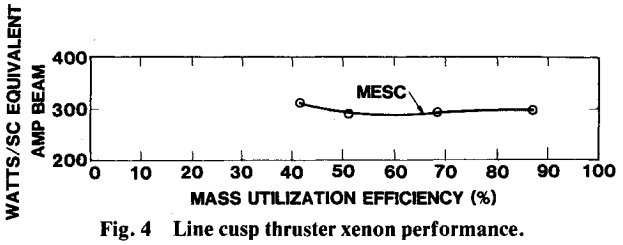

Fig. 4 Line cusp thruster xenon performance.

anode magnetic field tests may provide some insight into line cusp operation.

The first series of MESC configuration tests was conducted with the anodes all located in 10.0 mT fields. A factor of two greater current was collected at the upstream half of each anode. Also, a factor of five more current was collected by anodes in set 1 than in set 2. Locating anode sets 1 and 2 at 18.0 and 12.0 mT, respectively, produced a 1:1.3 electron current ratio between downstream and upstream anode halves and a 1.1:1 ratio between sets 1 and 2. These test data seemed to imply the plasma was selectively denser closer to every other anode in the upstream end of the discharge chamber.

Other tests at the same magnetic field differences but higher fields, 24.0 and 18.0 mT, produced unstable operation, while setting all anodes at 18.0 mT degraded performance. Attempts to reduce anode area by disconnecting either set of anodes degraded performance and increased anode operating potential.

Line cusp shell anode tests confirmed the asymmetric plasma distribution. The shell anode configuration showed a deterioration in performance with sustained argon operation above 225 W discharge power. Post-test examination found the magnets located at the upstream end of the discharge chamber, with opposite cathode magnet polarity, had been thermally demagnetized by the tests. Magnets in the same region with cathode magnet polarity showed no signs of damage.

Xenon operation of the shell anode configuration had similar results. Operation at ~150 W discharge produced the same magnet thermal demagnetization pattern.

Ring Cusp Thruster Performance

Figure 5 and 6 plot the ring cusp thruster performance of the MESC and shell anode configurations using the 0.17 T alnico magnets. The MESC configuration argon performance averaged ~70 W/SCE ampere beam less power consumption than the shell anode. A similar difference was seen in xenon operation where MESC averaged ~80 W/SCE ampere beam less.

Two MESC anode configurations were tested. The anodes were located in 12.5 mT average fields in the first series and 14.8 mT average fields in the second. Both started easily and operated stably. Moving the anode to the 14.8 mT field produced the best performance reducing discharge power consumption 30 W/SCE ampere beam.

A four-ring cusp shell anode configuration produced the best 0.17 T magnet performance. Tests were conducted with

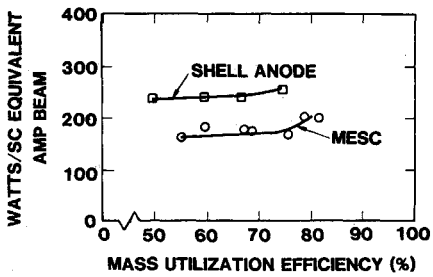

Fig. 5 Ring cusp argon performance, 0.17 T magnets.

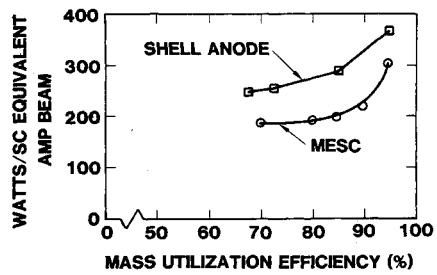

Fig. 6 Ring cusp xenon performance, 0.17 T magnets.

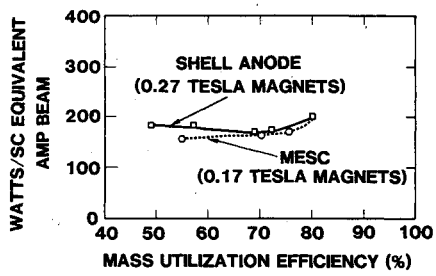

Fig. 7 Ring cusp argon performance.

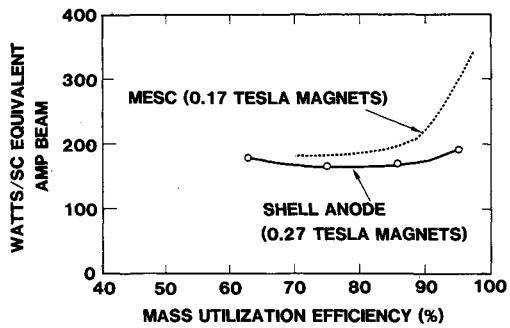

Fig. 8 Ring cusp xenon performance.

6, 4, and 2 cusps. Best performance was obtained with an uneven spaced 4-cusp pattern.

In the original 4-cusp pattern, the 0.17 T magnet rings were located 0.25, 2.8, 5.4, and 7.9 cm upstream from the grid mounting flange. Discharge probe data indicated the 7.9 cm upstream cusp collected an ion current density 1.4 times greater than average. Relocating the magnet rings 0.25, 3.0, 5.6, and 7.1 cm upstream of the mounting flange produced a fairly uniform ion current density to the probes and the best performance.

Figures 7 and 8 are plots of the performance achieved with the 2-cusp samarium-cobalt (Sm-Co) magnet assembly. Performance of the MESC ring cusp thruster fitted with alnico magnets have been reproduced for reference.

Two Sm-Co magnet patterns were evaluated during the shell anode tests. The 4-cusp pattern was similar to the uneven axial spacing mentioned above. The 2-cusp pattern was created by removing the second and third cusps upstream from the flange and moving the cusp next to the grids 1.5 cm upstream. The 2-cusp array produced the best performance.

Figure 7 shows the argon performance of the MESC and shell anode configurations were essentially the same. The MESC configuration, with the 0.17 T magnets, generated 76% argon utilization at 169 W/SCE ampere beam. The 0.27 T magnet shell anode assembly produced the same utilization at 177 W/SCE ampere beam.

Xenon performance of the two configurations shown in Fig. 8 was notably different. The MESC 0.17 T magnets assembly consumed more discharge power than the shell anode with 0.27 T magnets. The difference ranged from 20 to 110 W/SCE ampere beam at mass utilization efficiencies of 70-95%, respectively.

Discharge Chamber Probe Data

The array of probes in the ring cusp-shell anode discharge chamber measured the approximate ion current distribution during ring cusp-shell anode tests. In operation, they were usually biased 30 V negative of the cathode. Probe current densities were computed as the measured ion currents divided by the probe area.

The unevenly spaced, 4-cusp, alnico magnet shell anode test had wall probes 1.43, 4.20, and 6.3 cm upstream of the grid mounting flange. Probes over the magnets were 3.0, 5.6, and 7.1 cm upstream. Typical argon operation at a beam current density of 6.9 mA/cm^2 had mean wall probe ion current density of 0.9 mA/cm^2 and mean magnet probe current density of 4.6 mA/cm^2, or a ratio of 1:5. Increases or decreases in beam current density produced a similar change in probe current density but little change in the distribution current ratio.

Replacing the alnico magnet in the shell anode with Sm-Co magnets had a major impact on ion current distribution. Samarium-cobalt test data showed mean ion current densities of 0.25 and 4.0 mA/cm^2 were collected by the wall and magnet probes, respectively. This 1:16 ratio was about a factor three greater than the alnico magnet test recorded at similar thruster operating parameters. The Sm-Co assembly apparently had better ion containment.

Conclusions

The ring cusp thruster achieved noteworthy performance with both anode configurations. MESC configuration argon tests achieved 76% mass utilization at ~180 W/SCE ampere beam. The shell anode configuration fitted with stronger magnets achieved similar performance.

Substituting stronger magnets into the shell anode configuration made a major performance impact on thruster operation. Comparing argon shell anode performance at 75% utilization found that changing from 0.17 to 0.27 T magnets reduced discharge power consumption 47%.

Xenon operation saw similar changes with the magnet substitution. Changing magnets reduced discharge power consumption almost a factor of 2 at 90% utilization.

Both anode configuration tests with the line cusp thruster did not have the level of performance seen with the ring cusp type. It remains an open question if these results were inherent to the line cusp magnet design or apply only to the particular thruster tested. Poor performance was associated with axial and azimuthal asymmetric plasma distribution. It was not clear if the changes in the magnet pattern needed to overcome these problems would produce thruster performance that would equal the ring cusp results.

Acknowledgment

This work was supported by NASA Lewis Research Center under Contract NAS3-22876.

References

[1] Ramsey, W. D., "12-cm Argon-Xenon Ion Source," *Journal of Spacecraft and Rockets*, Vol. 16, July 1979, pp. 252-257.

[2] Ramsey, W. D., "Magnetoelectrostatic Thruster Physical Geometry Tests," *Journal of Spacecraft and Rockets*, Vol. 19, March 1982, pp. 133-138.

[3] Moore, R. D., "Magnetoelectrostatically Contained Ion Thruster," AIAA Paper 69-260, March 1969.

[4] Worlock, R. M., James, E. L., Hunter, R. E., and Bartlett, R.O., "ATS-6 North-South Stationkeeping Experiment," *IEEE Transactions on Aerospace and Electronic Systems*, Vol. AES-11, Nov. 1975, pp. 1176-1183.

[5] Ramsey, W. D., "12-cm Magneto-Electrostatic Containment Mercury Ion Thruster Development," *Journal of Spacecraft and Rockets*, Vol. 9, May 1972, pp. 318-321.

[6] Sovey, J. S., "Performance of a Magnetic Multipole Line Cusp Ion Thruster," AIAA Paper 81-0745, April 1981.

[7] Sovey, J. S., "Improved Ion Containment Using a Ring-Cusp Ion Thruster," AIAA Paper 82-1928, Nov. 1982.

[8] Vahrenkamp, R. P., "Measurement of Double Charged Ion in the Beam of a 30-cm Mercury Bombardment Thruster," AIAA Paper 73-1057, Oct. 1973.

[9] Kaufman, H. R. and Robinson, R. S., "Inert Gas Thrusters," NASA CR-159813, Nov. 1979.

[10] Holmes, A. J. T., "Role of Anode Area in the Behavior of Magnetic Multiple Discharge," *Review of Scientific Instruments*, Vol. 52, Dec. 1981, pp. 1814-1823.